



**AFRL-RQ-WP-TR-2016-0108**

**SILICON CARBIDE (SiC) DEVICE AND MODULE  
RELIABILITY**

**Performance of a Loop Heat Pipe Subjected to a Phase-Coupled Heat  
Input to an Acceleration Field**

**Kirk L. Yerkes (AFRL/RQQI) and James D. Scofield (AFRL/RQQE)**

**Flight Systems Integration Branch (AFRL/RQQI)**

**Electrical Systems Branch (AFRL/RQQE)**

**Power and Control Division**

**MAY 2016**

**Final Report**

**Approved for public release. Distribution is unlimited.**

*See additional restrictions described on inside pages*

**AIR FORCE RESEARCH LABORATORY  
AEROSPACE SYSTEMS DIRECTORATE  
WRIGHT-PATTERSON AIR FORCE BASE, OH 45433-7541  
AIR FORCE MATERIEL COMMAND  
UNITED STATES AIR FORCE**

## NOTICE AND SIGNATURE PAGE

Using Government drawings, specifications, or other data included in this document for any purpose other than Government procurement does not in any way obligate the U.S. Government. The fact that the Government formulated or supplied the drawings, specifications, or other data does not license the holder or any other person or corporation; or convey any rights or permission to manufacture, use, or sell any patented invention that may relate to them.

This report was cleared for public release by the USAF 88th Air Base Wing (88 ABW) Public Affairs Office (PAO) and is available to the general public, including foreign nationals.

Copies may be obtained from the Defense Technical Information Center (DTIC)  
(<http://www.dtic.mil>).

AFRL-RQ-WP-TR-2016-0108 HAS BEEN REVIEWED AND IS APPROVED FOR PUBLICATION IN ACCORDANCE WITH ASSIGNED DISTRIBUTION STATEMENT.

*\*//Signature//*

---

JAMES D. SCOFIELD  
Program Manager  
Electrical Systems Branch  
Power and Control Division

*//Signature//*

---

GREGORY L. FRONISTA, Chief  
Electrical Systems Branch  
Power and Control Division  
Aerospace Systems Directorate

*//Signature//*

---

BRYAN J. CANNON, Principal Scientist  
Power and Control Division  
Aerospace Systems Directorate

This report is published in the interest of scientific and technical information exchange and its publication does not constitute the Government's approval or disapproval of its ideas or findings.

\*Disseminated copies will show "*//Signature//*" stamped or typed above the signature blocks.

<b>REPORT DOCUMENTATION PAGE</b>				<i>Form Approved</i> OMB No. 0704-0188	
<p>The public reporting burden for this collection of information is estimated to average 1 hour per response, including the time for reviewing instructions, searching existing data sources, gathering and maintaining the data needed, and completing and reviewing the collection of information. Send comments regarding this burden estimate or any other aspect of this collection of information, including suggestions for reducing this burden, to Department of Defense, Washington Headquarters Services, Directorate for Information Operations and Reports (0704-0188), 1215 Jefferson Davis Highway, Suite 1204, Arlington, VA 22202-4302. Respondents should be aware that notwithstanding any other provision of law, no person shall be subject to any penalty for failing to comply with a collection of information if it does not display a currently valid OMB control number. <b>PLEASE DO NOT RETURN YOUR FORM TO THE ABOVE ADDRESS.</b></p>					
<b>1. REPORT DATE (DD-MM-YY)</b> May 2016		<b>2. REPORT TYPE</b> Final		<b>3. DATES COVERED (From - To)</b> 01 October 2014 – 30 January 2016	
<b>4. TITLE AND SUBTITLE</b> SILICON CARBIDE (SiC) DEVICE AND MODULE RELIABILITY Performance of a Loop Heat Pipe Subjected to a Phase-Coupled Heat Input to an Acceleration Field				<b>5a. CONTRACT NUMBER</b> In-house	
				<b>5b. GRANT NUMBER</b>	
				<b>5c. PROGRAM ELEMENT NUMBER</b> 62203F	
<b>6. AUTHOR(S)</b> Kirk L. Yerkes (AFRL/RQQI) James D. Scofield (AFRL/RQQE)				<b>5d. PROJECT NUMBER</b> 3145	
				<b>5e. TASK NUMBER</b>	
				<b>5f. WORK UNIT NUMBER</b> Q0M5	
<b>7. PERFORMING ORGANIZATION NAME(S) AND ADDRESS(ES)</b> Flight Systems Integration Branch (AFRL/RQQI) Electrical Systems Branch (AFRL/RQQE) Power and Control Division Air Force Research Laboratory, Aerospace Systems Directorate Wright-Patterson Air Force Base, OH 45433-7541 Air Force Materiel Command, United States Air Force				<b>8. PERFORMING ORGANIZATION REPORT NUMBER</b> AFRL-RQ-WP-TR-2016-0108	
<b>9. SPONSORING/MONITORING AGENCY NAME(S) AND ADDRESS(ES)</b> Air Force Research Laboratory Aerospace Systems Directorate Wright-Patterson Air Force Base, OH 45433-7541 Air Force Materiel Command United States Air Force				<b>10. SPONSORING/MONITORING AGENCY ACRONYM(S)</b> AFRL/RQQE	
				<b>11. SPONSORING/MONITORING AGENCY REPORT NUMBER(S)</b> AFRL-RQ-WP-TR-2016-0108	
<b>12. DISTRIBUTION/AVAILABILITY STATEMENT</b> Approved for public release; distribution unlimited.					
<b>13. SUPPLEMENTARY NOTES</b> PA Case Number: 88ABW-2016-2399; Clearance Date: 12 May 2016. This is a work of the U.S. Government and is not subject to copyright protection in the United States.					
<b>14. ABSTRACT</b> The objective of this research was to experimentally investigate transient operating characteristics of a titanium-water loop heat pipe subjected to a phase-coupled heat input and acceleration field. The acceleration field was generated using a centrifuge table by varying the radial acceleration. Both evaporator heat input and radial acceleration were generated as periodic sine functions at a frequency, $f = 0.05$ Hz. Evaporator heat input and radial acceleration peak-to-peak values varied from $100 \text{ W} \leq Q_{in} \leq 700 \text{ W}$ and $3.0 \text{ g} \leq a_r \leq 10 \text{ g}$ , respectively. The radial acceleration sine function was initiated either at the same time as the evaporator heat input function or delayed resulting in varying phase angles, $\phi = 0^\circ, 180^\circ,$ and $270^\circ$ . The inlet condenser cold plate coolant temperature were varied at $T_{cp} = 45^\circ \text{C}, 50^\circ \text{C},$ and $60^\circ \text{C}$ . The rejected heat from the condenser was measured over time and compared to a first-order thermal system. It was found that energy was dissipated in the condenser as a second-order phenomena and varied with phase evaporator heat input and acceleration field phase angle and condenser input temperature. The equivalent time constant tended to decrease with increasing phase angle and decreasing condenser inlet temperature while the delay time increased with increasing phase angle and decreasing condenser inlet temperature.					
<b>15. SUBJECT TERMS</b> silicon carbide, power electronics thermal management, design of experiments					
<b>16. SECURITY CLASSIFICATION OF:</b>			<b>17. LIMITATION OF ABSTRACT:</b> SAR	<b>18. NUMBER OF PAGES</b> 19	<b>19a. NAME OF RESPONSIBLE PERSON (Monitor)</b> James D. Scofield <b>19b. TELEPHONE NUMBER (Include Area Code)</b> N/A
<b>a. REPORT</b> Unclassified	<b>b. ABSTRACT</b> Unclassified	<b>c. THIS PAGE</b> Unclassified			

## Table of Contents

<b>Section</b>	<b>Page</b>
List of Figures .....	ii
List of Tables .....	ii
Abstract .....	iii
1. Introduction .....	1
2. Experimental Approach .....	2
3. Results and Discussion .....	7
4. Conclusion .....	11
5. References .....	12
Nomenclature .....	13

## List of Figures

<b>Figure</b>	<b>Page</b>
Figure 1. Experimental Schematics .....	4
Figure 2. Radial, $a_{rLHP} = 1-10g$ , and Axial, $a_{zLHP}$ , Acceleration Components .....	6
Figure 3. Radial Acceleration and Input Heat Load Showing a $270^\circ$ Phase Angle .....	8
Figure 4. Rejected Heat Load from the LHP Condenser and Fitted First-order Exponential Function .....	8
Figure 5. Plotted Phase Angle .....	10

## List of Tables

<b>Table</b>	<b>Page</b>
Table 1. Titanium-water LHP Design Parameters .....	3
Table 2. Centrifuge Run Parameter Settings and Results .....	9

## Abstract

The objective of this research is to experimentally investigate the transient operating characteristics of a titanium-water loop heat pipe subjected to a phase-coupled evaporator heat input and acceleration field. The acceleration field was generated using a centrifuge table by varying the radial acceleration. Both evaporator heat input and radial acceleration were generated as periodic sine functions at a frequency,  $f = 0.05$  Hz. Evaporator heat input and radial acceleration peak-to-peak values varied from  $100 \text{ W} \leq Q_{in} \leq 700 \text{ W}$  and  $3.0 \text{ g} \leq a_r \leq 10 \text{ g}$  respectively. The radial acceleration sine function was initiated either at the same time as the evaporator heat input function or delayed resulting in varying phase angles,  $\phi = 0^\circ, 180^\circ,$  and  $270^\circ$ . The inlet condenser cold plate coolant temperature were varied at  $T_{cp} = 45^\circ\text{C}, 50^\circ\text{C},$  and  $60^\circ\text{C}$ . The rejected heat from the condenser was measured over time and compared as a first-order thermal system with a time constant and delay. It was found that energy was dissipated in the condenser as a second-order phenomena and varied with phase evaporator heat input and acceleration field phase angle and condenser input temperature. The equivalent time constant tended to decrease with increasing phase angle and decreasing condenser inlet temperature while the delay time increased with increasing phase angle and decreasing condenser inlet temperature.

## 1. Introduction

The loop heat pipe (LHP), due to its passive heat transport capability, is one potential solution for a variety of aircraft thermal management challenges such as cooling power electronics components. At best, the LHP represents the transport of heat due to the complex interaction of numerous thermodynamics forces<sup>1</sup>. Its operation can embody a variety of dynamical responses when perturbed by driving forces such as evaporator input heat rate load and temperatures of the condenser and compensation chamber<sup>2</sup>. In addition, the LHP can also be sensitive to external body forces, such as transitory acceleration induced forces, that may alter the LHP dynamical performance and stability. Typically, the LHP has been assumed to be insensitive to acceleration induced forces due to the design and wicking properties of the discrete capillary structure within the evaporator. Ku et al.<sup>8,9</sup> studied the effect of the acceleration induced forces on the LHP operating temperatures. When a centrifugal force was applied to the LHP, it was found that steady-state acceleration induced forces altered liquid/vapor distributions within the LHP which significantly influenced its performance and temperature oscillation.

The physical meaning of and subsequent LHP performance resulting from acceleration induced forces on the condenser operation is not well understood. It is suspected that with combined heat input and elevated acceleration, competing thermodynamic forces and steady-state acceleration induced forces must balance allowing the LHP to either operate or fail. At best, the normal performance of a LHP involves complex coupled thermodynamics associated with fluid thermal properties and thermodynamic forces throughout the LHP. In an accelerating environment, steady-state or transitory, the prediction of LHP performance is difficult without a thorough understanding as to the nature of competing or complementing thermodynamic induced forces with acceleration induced forces across the entire LHP.

Fleming et al.<sup>10</sup> and Yerkes et al.<sup>11</sup> investigated performance of a titanium-water LHP mounted on a centrifuge and subjected to elevated steady-state and steady-period acceleration fields. These preliminary experimental investigations defined the steady-state and transitory operating characteristics of the LHP subjected to a combined steady-state input heat rate and elevated steady-state and steady-period acceleration fields.

This study experimentally investigates the transient operating characteristics of a titanium-water loop heat pipe subjected to a phase-coupled evaporator heat input and acceleration field. Both evaporator heat input and radial acceleration were generated as periodic sine functions at a fixed frequency. The radial acceleration was delayed and phase-shifted from the evaporator heat input to evaluate transitory performance and failure conditions of the LHP.

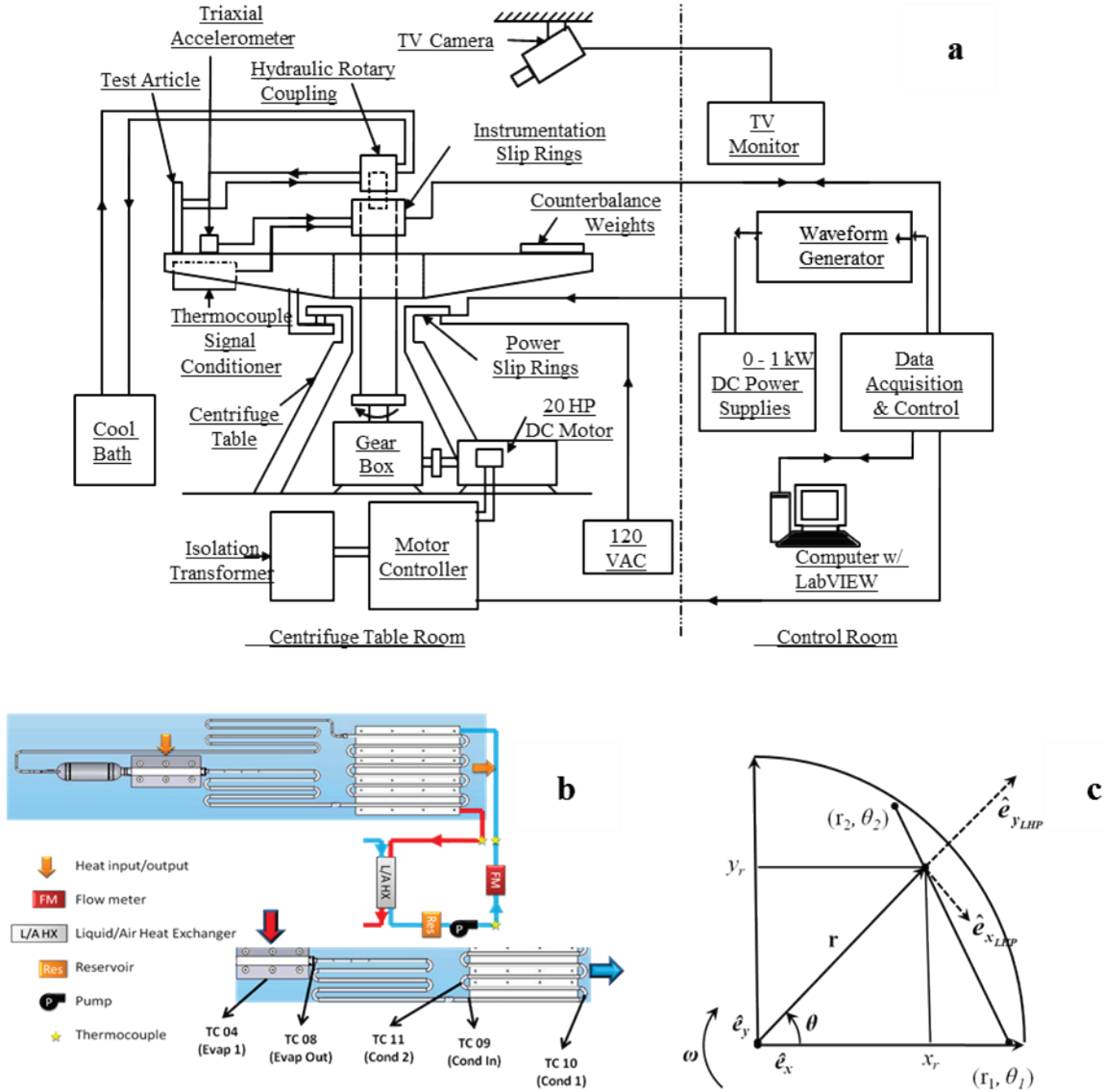
## 2. Experimental Approach

Table 1 shows the titanium-water LHP design parameters as studied by Fleming et al.<sup>10</sup> and Yerkes et al.<sup>11</sup> and used in this research. Figure 1 schematically shows the experimental apparatus consisting of a 2.44-m horizontal centrifuge table and the titanium-water LHP. Power and instrumentation signals were passed through separated rotational slip rings to minimize electrical noise and interference. Transient acceleration measurements were made using a rectangular coordinate system orthogonal triaxial Columbia (model SA-307HPTX) accelerometer with an uncertainty of  $\pm 0.01g$ . The accelerometer was mounted such that the radial acceleration component was aligned with y-axis. The accelerometer output was consistent with a right-hand coordinate system with the y-axis and x-axis mounted in the radial direction and the tangential direction respectively. To ensure proper control of the centrifuge table during the experiments, radial acceleration profiles were digitally generated, stored on a Fluke Waveform Generator (Model 292), and integrated into a LabView data acquisition and control program for the centrifuge table.

For this experimental investigation, an intermediate water coolant loop supplied coolant to the cold plate heat sink mounted to the LHP condenser. A Tek Temp cool bath, consisting of a pump, reservoir, and liquid-air heat exchanger, was operated external to the centrifuge in order to provide sufficient temperature control of the water coolant to maintain the cold plate inlet temperature,  $T_{cp}$ . Water coolant flow, from the cool bath, was supplied to the centrifuge through the use of a rotating hydraulic slip ring. The cold plate coolant flow rate was measured and maintained at  $0.077\text{kg/s}$ , with an uncertainty to within 5%, using a calibrated Sponsler (model SP 711-3) flow meter mounted on the centrifuge table. Figure 1 also schematically illustrates the titanium-water LHP and thermocouple locations monitored during the experiments and the coordinate reference frame convention used to analyze the acceleration vector field.

**Table 1. Titanium-water LHP Design Parameters**

<b><u>Requirement</u></b>	<b><u>Parameter</u></b>
<b><u>Thermal</u></b>	
Minimum Heat Load	500W
Minimum Heat Flux	3W/cm <sup>2</sup>
Maximum Operating Temperature	200°C
Condenser Heat Sink Temperature	5 to 140°C
Tilt in One G	± 0in, horizontal
Conductance	50°C/W
Proof of Pressure Test	3102 psi (200°C)
<b><u>Materials</u></b>	
Evaporator Envelope Material	Titanium, CP Grade 2
Primary Wick Material	Titanium, CP Grade 2
Secondary Wick Material	Titanium, CP Grade 2
Transport Line Material	Titanium, CP Grade 2
Working Fluid	Water
Fluid Charge	300mL
<b><u>LHP Dimensions</u></b>	
Evaporator Footprint	20.32 × 10.16cm <sup>2</sup>
Condenser Footprint	30.48 × 28.58cm <sup>2</sup>
Vapor Line Length	Approx. 243.8cm
Vapor Line Diameter	0.9525 OD × 0.0889cm wall
Liquid Line Length	Approx. 335.3cm
Liquid Line Diameter	0.6350 OD × 0.0889cm wall
Condenser Line Length	Approx. 279.4cm
Condenser Line Diameter	0.9525 OD × 0.0889cm wall
<b><u>Compensation Chamber</u></b>	
Diameter	6.033cm OD
Length	11.43cm
Chamber Location	Coaxial with evaporator
<b><u>Primary Wick Properties</u></b>	
Effective Pore Radius	9.1micron
Permeability	1.2×10 <sup>-12</sup> m <sup>2</sup>
Outside Diameter	2.286cm
Length	20.32cm
Inside Diameter	0.8001cm
Number of Grooves	6
Groove Depth	0.1524cm
Groove Width	0.1524cm
<b><u>Secondary Wick Properties</u></b>	
Mesh	150 × 150



**Figure 1. Experimental Schematics**

(The schematic shows (a) the centrifuge, (b) the titanium-water loop heat pipe experimental setup, and (c) the centrifuge and accelerometer coordinate system corresponding to the condenser mounting location.

For these experiments, the time variant radial acceleration and input heat load were controlled as a sine wave function of the form,  $\omega^2 R_{ref} = A \sin 2\pi ft + B$  and  $Q_{in} = C \sin 2\pi ft + D$  respectively. The acceleration, while accounting for the clockwise rotation of the centrifuge, the angular velocity vector becomes

$$\boldsymbol{\omega} = -\omega \hat{\mathbf{e}}_z = -\sqrt{\frac{(A \sin 2\pi ft + B)}{R_{ref}}} \hat{\mathbf{e}}_z, \quad (1)$$

where

$$A = \left( \frac{a\Gamma_{high} - a\Gamma_{low}}{2} \right),$$

$$B = \left( \frac{a\Gamma_{high} + a\Gamma_{low}}{2} \right),$$

and

$$\frac{d\omega}{dt} = -\frac{A\pi f \cos 2\pi ft}{\sqrt{R_{ref} (A \sin 2\pi ft + B)}} \hat{e}_z \quad (2)$$

where the effective acceleration is of the form

$$\begin{aligned} \mathbf{a}_{eff} &= at\hat{e}_{xLHP} + ar\hat{e}_{yLHP} + az\hat{e}_z = r\frac{d\omega}{dt}\hat{e}_{xLHP} + r(-\omega)^2\hat{e}_{yLHP} + (-g)\hat{e}_z \\ &= \left\{ \left( \frac{r_1}{\left( \frac{(\sin \theta)(r_1 - r_2 \cos \theta_2)}{r_2 \sin \theta_2} + \cos \theta \right)} \right) \left( -\frac{A\pi f \cos 2\pi ft}{\sqrt{R_{ref} (A \sin 2\pi ft + B)}} \right) \right\} \hat{e}_{xLHP} \\ &\quad + \left\{ \left( \frac{(A \sin 2\pi ft + B)}{R_{ref}} \right) \left( \frac{r_1}{\left( \frac{(\sin \theta)(r_1 - r_2 \cos \theta_2)}{r_2 \sin \theta_2} + \cos \theta \right)} \right) \right\} \hat{e}_{yLHP} \\ &\quad + (-g)\hat{e}_z. \end{aligned} \quad (3)$$

As discussed by Yerkes et al.<sup>11</sup>, to determine acceleration field within the LHP, the coordinate system  $\hat{e}_{xLHP}, \hat{e}_{yLHP}, \hat{e}_z$ , as shown by Eq. 3, can be rotated to align with the radial and axial coordinates,  $\hat{e}_{rLHP}, \hat{e}_{zLHP}, \hat{e}_z$ , of the LHP. (Note, the radial acceleration component as described is really a transverse acceleration component generated by a combination of the radial and tangential acceleration components due to the centrifuge dynamics. For this discussion, this component is acting normal to the centerline of the LHP.)

Similarly, the input heat load was generated at the same frequency as the acceleration, where

$$C = \left( \frac{Q_{high} - Q_{low}}{2} \right) \text{ and}$$

$$D = \left( \frac{Q_{high} + Q_{low}}{2} \right).$$

Temperature measurements were made using both calibrated type-T and type-E thermocouples with an uncertainty of  $\pm 0.05^\circ\text{C}$ . All of the low voltage thermocouple outputs were preconditioned and amplified on the centrifuge to minimize losses through the instrumentation slip ring. Bare thermocouple beads were mounted in place with thermal grease and secured with Kapton tape.

The evaporator input heat rate to the LHP was provided using a mica heater (Minco) mounted on the evaporator and powered from the output of a Kepco (model ATE-150-7M) power supply. Evaporator heater power was determined from voltage measurements across a precision resistor, in series with the evaporator heater, with an uncertainty of  $\pm 2.0\%$ .

During the LHP operation, the compensation chamber was insulated without additional heating or cooling. Thermocouples were mounted around the centerline circumference of the

compensation chamber to measure any temperature variation as a result of fluid slosh due to induced accelerations. The LHP was mounted in such a manner as to minimize the radial variation along the length of the LHP. The vapor and liquid lines were bent to maintain the radius of curvature of the centrifuge. However, the condenser/cold plate and evaporator/compensation chamber varied in radial location due to their linear construction. This introduced an acceleration gradient along the length of the condenser/cold plate and evaporator/compensation chamber as discussed by Yerkes et al.<sup>11</sup> and shown in Figure 2.

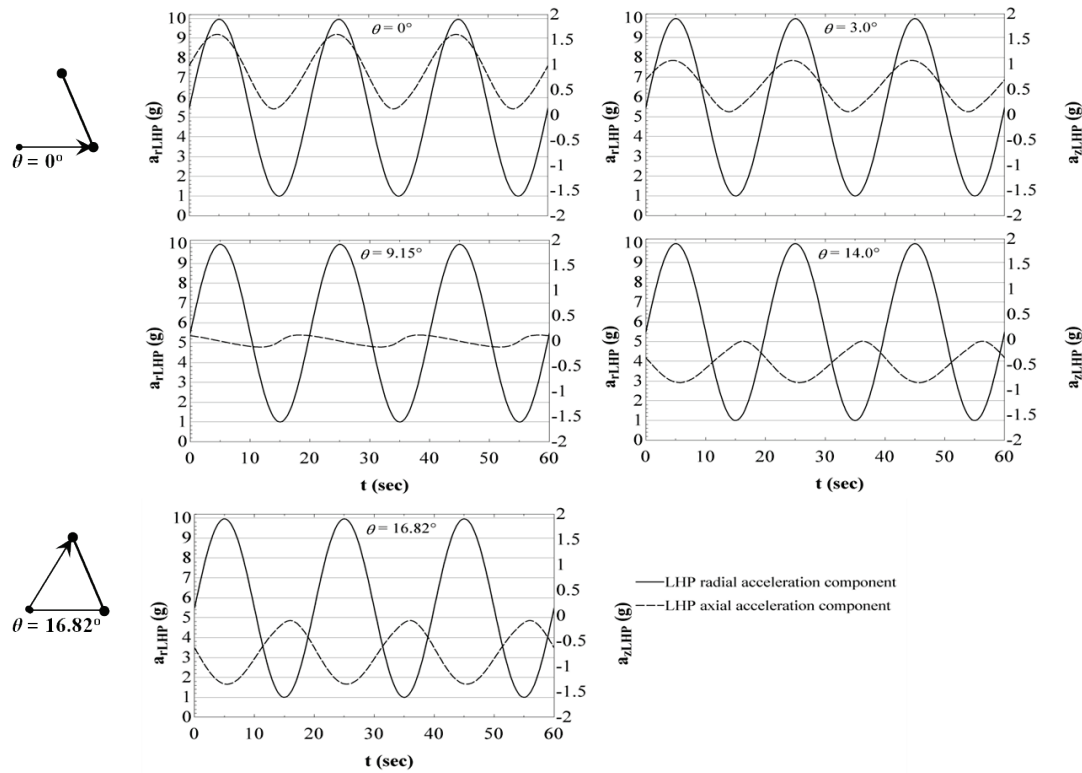


**Figure 2. Radial,  $a_{r,LHP} = 1-10g$ , and Axial,  $a_{z,LHP}$ , Acceleration Components**

*(The components are referenced to the LHP condenser for varying position vector angle,  $\theta$ . (Yerkes et al.<sup>11</sup>.)*

### 3. Results and Discussion

The acceleration field was generated, using the centrifuge table described, by varying the radial acceleration. The inlet condenser cold plate coolant temperature were varied at  $T_{cp} = 45\text{ }^{\circ}\text{C}$ ,  $50\text{ }^{\circ}\text{C}$ , and  $60\text{ }^{\circ}\text{C}$ . Both radial acceleration and evaporator heat input were generated as periodic sine functions at a frequency,  $f = 0.05\text{Hz}$ . Evaporator heat input and radial acceleration peak-to-peak values varied from  $100\text{ W} \leq Q_{in} \leq 700\text{ W}$  and  $3.0\text{ g} \leq a_r \leq 10\text{ g}$ , respectively. The radial acceleration sine function was initiated either at the same time as the evaporator heat input function or delayed resulting in varying phase angles,  $\phi = 0^{\circ}$ ,  $180^{\circ}$ , and  $270^{\circ}$ . Figure 3 shows the Radial acceleration and input heat load showing a  $270^{\circ}$  phase angle. Figure 4 shows the rejected heat load from the condenser measured over time and a fitted exponential assuming the reponse as a first-order thermal system with a time constant and delay. Taking the difference between the integrated the rejected condenser heat load and the integrated fitted first-order exponential function, over time, results in the effective energy lost in the condenser. This is most likely due to PdV work on the fluid in the vapor line to move the liquid into the condenser during start-up.

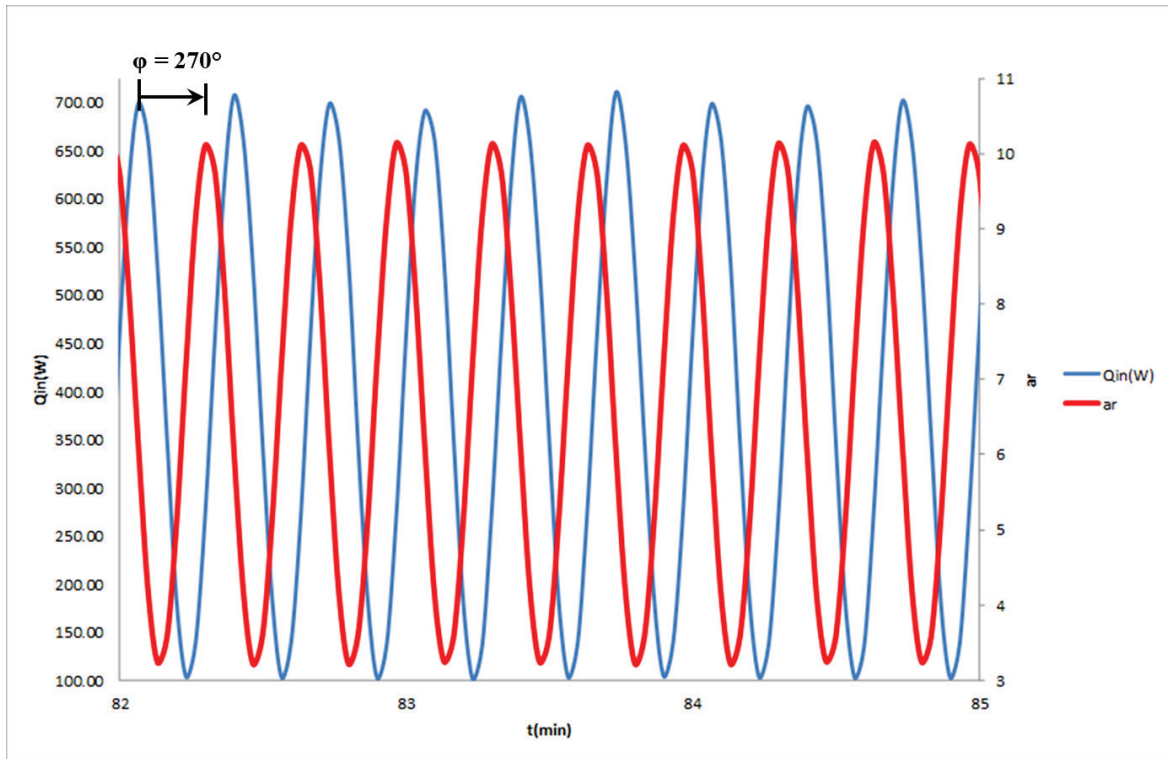


**Figure 3. Radial Acceleration and Input Heat Load Showing a 270° Phase Angle**  
*(Upon startup, the input heat load precedes radial acceleration.)*

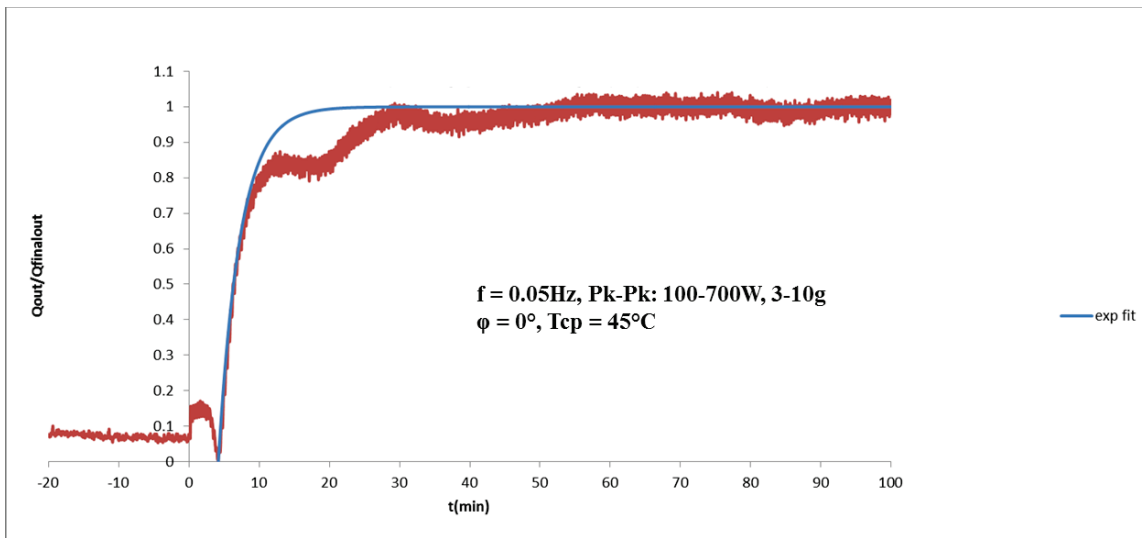


**Figure 4. Rejected Heat Load from the LHP Condenser and Fitted First-order Exponential Function**

Table 2 tabulates the fitted exponential time constant, delay time, run/fail conditions as related to the input phase angle,  $\phi$ , and condenser temperature,  $T_{cp}$ . Figure 5 plots the results shown in Table 2 highlighting the runs that, over time, led to failure. Also shown is the normalized energy difference assuming the first order response, exponential fit, would be the

response if no energy was expended in the condenser. The normalized energy difference is the difference in the integrated results between this first order response and the energy removed from the condenser and represents the relative change of energy expended in the condenser during the LHP transitory operation.

In general, the time constant and sum of the time constant and delay time decreased with increasing phase angle while the delay time increased with increasing phase angle. The condenser temperature,  $T_{cp}$ , also appeared to influence the time constant and delay time where the time constant and sum of the time constant and delay time decreased with decreasing  $T_{cp}$  while the delay time increased with decreasing  $T_{cp}$ . The normalized energy difference, appeared to decrease with increased phase angle and decreased  $T_{cp}$ . The exception to this was at the 180° phase angle with a  $T_{cp} = 50\text{ }^{\circ}\text{C}$  and  $60\text{ }^{\circ}\text{C}$ .

The observed failure, of the LHP to operate, tended to occur after the LHP appeared to operate for an hour or more. Both phase angle and condenser temperature,  $T_{cp}$ , appeared to influence the time for LHP failure to occur. This may be due, in part, to the natural frequency of the fluid motion internal to the condenser being influenced, over time, by the induced forces resulting from the driving frequency of the acceleration coupled to the frequency of the of input heat load.

**Table 2. Centrifuge Run Parameter Settings and Results**

<b>Phase Angle (deg)</b>	<b><math>T_{cp}</math> (deg C)</b>	<b>Time Constant (sec)</b>	<b>Delay Time (sec)</b>	<b>Ran/Failed</b>	<b>Time to Fail (min)</b>
270	50	171	256	failed	90
0	50	210	249	ran	-
180	50	184	258	ran	-
180	45	168	260	failed	65
0	45	187	250	failed	130
180	60	250	242	ran	-

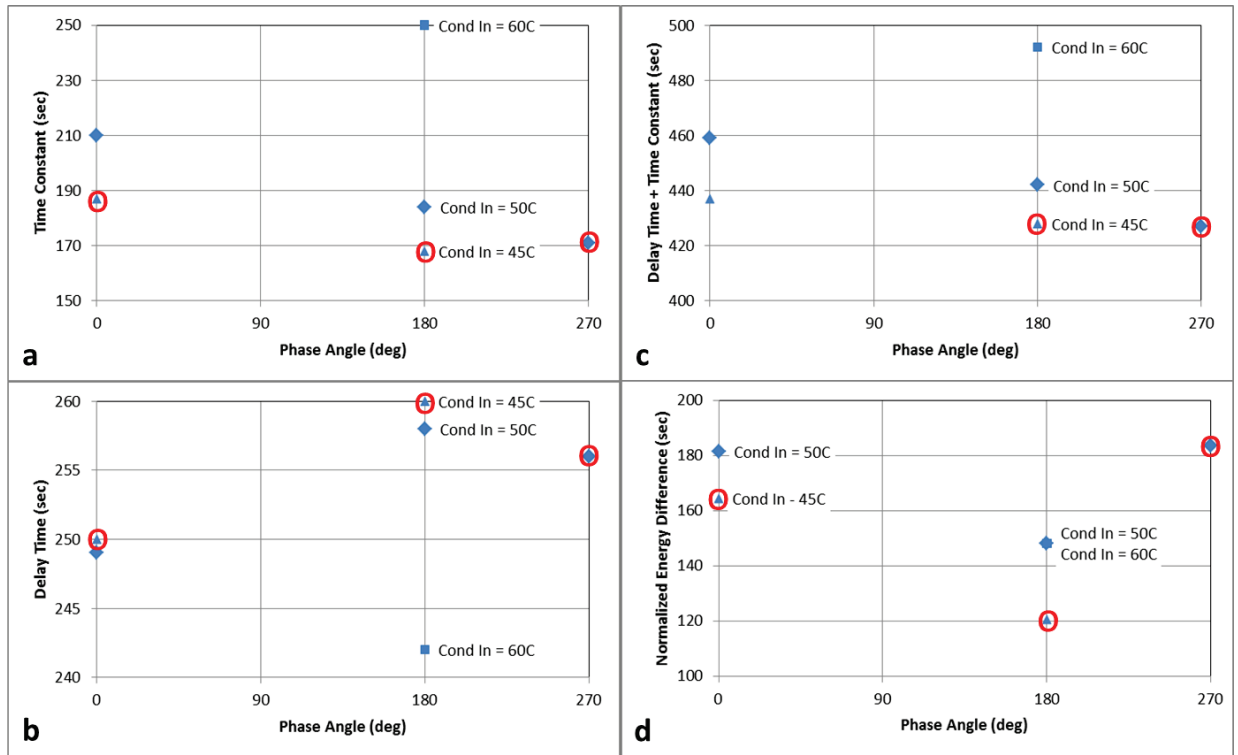


**Figure 5. Plotted Phase Angle**

*(The plot shows time constant, delay time, and normalized energy difference results (highlighted runs, over time, led to failure).)*

#### 4. Conclusion

Dynamic forces generated from acceleration transients, when combined with thermodynamic forces, can significantly impact the dynamical performance of a LHP. This is particularly true when dynamic acceleration driven forces are phase-coupled to the dynamic heat generation. For this investigation, the transient operating characteristics of a titanium-water loop heat pipe were observed when subjected to a phase-coupled evaporator heat input to acceleration field at varying condenser temperatures. Both evaporator heat input and acceleration were generated as periodic sine functions at a fixed frequency. The acceleration was delayed and phase-shifted from the evaporator heat input to evaluate dynamical performance and failure conditions of the LHP. The LHP performance appears to be due, in part, to the natural frequency of the fluid motion internal to the condenser resulting from the driving frequency of the acceleration phase-coupled to the frequency of the of input heat load. This effected the LHP time constant, delay time, and in some cases led to delayed failure. It is clear that one should clearly understand the nature of the resulting forces, i.e., magnitude and direction, which are generated from a transitory and spatial acceleration vector field and their impact on the dynamical performance of two-phase thermodynamic systems such as LHPs.

## 5. References

- [1] Ku, J., "Operating characteristics of Loop Heat Pipes," SAE Paper 1999-01-2007, July 1999.
- [2] Ku, J., Ottenstein, L., Kobel, M., Rogers, P., Kaya, T., "Temperature Oscillations in Loop Heat Pipe Operation," AIP Conf. Proc. Vol. 552, 2001, pp. 255; DOI: 10.1063/1.1357932.
- [3] Bai, L., Lin, G., Zhang, H., Wen, D., "Mathematical Modeling of Steady-State Operation of a Loop Heat Pipe," Applied Thermal Engineering, Vol. 29, No. 13, 2009, pp. 2643-2654.
- [4] Bai, L., Lin, G., Wen, D., "Modeling and Analysis of Startup of a Loop Heat Pipe," Applied Thermal Engineering, Vol. 30, No. 17-18, 2010, pp. 2778-2787.
- [5] Shukla, K., "Thermo-fluid dynamics of Loop Heat Pipe Operation," International Communications in Heat and Mass Transfer, Vol. 35, No. 8, 2008, pp. 916-920.
- [6] Khrustalev, D., "Advances in Transient Modeling of Loop Heat Pipe Systems with Multiple Components," AIP Conf. Proc. Vol. 1208, 2010, pp. 55; DOI: 10.1063/1.3326285.
- [7] Hoang, T., "Stability and Oscillations in Loop Heat Pipe Operations: A Classic Non-Linear Dynamics Problem," International Two-Phase Thermal Control Workshop, University of Maryland, 31 October 2011-3 November 2011.
- [8] Ku, J., Ottenstein, L., Kaya, T., Rogers, P., and Hoff, C., "Testing of a Loop Heat Pipe Subjected to Variable Accelerating Forces, Part1: Start-Up," SAE Paper 2000-0102488, July 2000.
- [9] Ku, J., Ottenstein, L., Kaya, T., Rogers, P., and Hoff, C., "Testing of a Loop Heat Pipe Subjected to Variable Accelerating Forces, Part2: Temperature Stability," SAE Paper 2000-0102489, July 2000.
- [10] Fleming, A., Thomas, S.K., Yerkes, K., "Titanium-Water Loop Heat Pipe Operating Characteristics Under Standard and Elevated Acceleration Fields," Journal of Thermophysics and Heat Transfer, Vol. 24, No. 1, 2010, pp.184-198; DOI: 10.2514/45684.
- [11] Yerkes, K., Scofield, J., Courson, D., and Jiang, H., "Steady-Periodic Acceleration Effects on the Performance of a Titanium-Water Loop Heat Pipe," Journal of Thermophysics and Heat Transfer, Vol. 28, No. 3, 2014, pp. 440-454; DOI: 10.2514/1.T3900.

## Nomenclature

$\mathbf{a}_{eff}$	effective acceleration vector field on the LHP
ar	radial acceleration component, g
at	tangential acceleration component, g
az	vertical acceleration component, g
$\hat{\mathbf{e}}$	coordinate axis unit vector
f	acceleration frequency, Hz
$\mathbf{g}$	acceleration vector due to gravity
g	acceleration vertical component due to gravity, g
Qin	input heat rate, W
$\mathbf{r}$	position vector
r	position vector radial coordinate, m
$R_{ref}$	reference position; accelerometer radial position, 1.208m (47.56in)
$r_1$	LHP condenser end radial location, 1.219m (48.0in)
$r_2$	LHP condenser end radial location, 1.215m (47.82in)
t	time, min or sec
T	temperature, °C
Tcp	cold plate coolant inlet temperature, °C
$z_r$	position vector vertical coordinate, m

### Greek

$\theta$	angular position of the position vector, degrees
$\theta_1$	angular position of the position vector at $r_1$ , 0°
$\theta_2$	angular position of the position vector at $r_2$ , 16.82°
$\boldsymbol{\omega}$	angular velocity vector
$\omega$	angular velocity vector component, rad/sec

### Subscripts

high	maximum
low	minimum
rLHP	radial component of the acceleration vector oriented on the LHP
yLHP	radial component of the acceleration vector oriented with the accelerometer
xLHP	tangential component of the acceleration vector oriented with the accelerometer
z	vertical component of the acceleration vector
zLHP	axial component of the acceleration vector oriented on the LHP